Biointerface Research in Applied Chemistry
Open-Access Journal (ISSN: 2069-5837)

Article
Volume 15, Issue 3, 2025, 40
https://doi.org/10.33263/BRIAC153.040

Radiosynthesis and Initial *In Vitro* Study of Radioiodinated-Labeled Oligo-Acidic Peptide Targeting Bone

Shafira Shafira [1], Nurmaya Effendi [2,*], Amal Rezka Putra [3], Faradiba Faradiba [4], Rien Ritawidya [5], Ahmad Najib [6], Kazuma Ogawa [7,*]

1 Postgraduate School, Master's School of Pharmacy, Universitas Muslim Indonesia, Makassar, Indonesia; 000212022022@umi.ac.id (S.S.);
2 Department of Pharmaceutical Chemistry, Faculty of Pharmacy, Universitas Muslim Indonesia, Makassar, Indonesia; nurmaya.effendi@umi.co.id (N.E.);
3 Research Center for Radioisotope, Radiopharmaceutical, and Biodosimetry Technology, National Research and Innovation Agency (BRIN), Tangerang Selatan, Indonesia; amal.rezka.putra@brin.go.id (A.R.);
4 Department of Apothecary, Faculty of Pharmacy, Universitas Muslim Indonesia, Makassar, Indonesia; faradiba.faradiba@umi.ac.id (F.F.);
5 Research Center for Radioisotope, Radiopharmaceutical, and Biodosimetry Technology, National Research and Innovation Agency (BRIN), Tangerang Selatan, Indonesia; rien001@brin.go.id (R.R.);
6 Department of Apothecary, Faculty of Pharmacy, Universitas Muslim Indonesia, Makassar, Indonesia; ahmad.najib@umi.ac.id (A.N.);
7 Graduate School of Medical Sciences, Kanazawa University, Kanazawa, Japan; kogawa@p.kanazawa-u.ac.jp (K.O.);
* Correspondence: nurmaya.effendi@umi.ac.id (N.E.) and kogawa@p.kanazawa-u.ac.jp (K.O.);

Received: 6.02.2025; Accepted: 10.05.2025; Published: 8.06.2025

Abstract: Radiolabeling of poly-aspartic acid potential becomes carriers to deliver diagnostic and therapeutic agents to the bone and showed a high affinity for hydroxyapatite, the dominant mineral in the bone. Recently, we designed and synthesized the radiotracers, [^{125}I]IB-D_8-OH ([^{125}I]**8**) and [^{125}I]IB-D_{11}-OH ([^{125}I]**9**), as well as in vitro evaluated their affinities for hydroxyapatite. The peptide was prepared using the solid-phase peptide synthesis method and linked with a prosthetic group, *N*-succinimidyl 3-(tri-n-butylstannyl)benzoate (ATE), to afford corresponding precursors for preparing radioiodinated peptides. The [^{125}I]**8** and [^{125}I]**9** were prepared using an iododestannylation reaction, with optimized labeling conditions by changing the reaction time and the temperature of the reaction. HPLC identified the labeled products, and their radiochemical yield, purity, stability in PBS(-), and affinity for hydroxyapatite were evaluated. The optimal labeling condition in this study used an oxidizing agent, *N*-chlorosuccinimide (NCS), which reacted for 15 minutes at room temperature in an acidic solution. This labeled method showed high labeling efficiency with radiochemical yield >94%, radiochemical purity >98%, and stable labeling. The [^{125}I]**8** and [^{125}I]**9** had a high affinity for hydroxyapatite. We developed [^{125}I]-labeled poly-aspartic acid peptide with high stability in PBS(-) and murine plasma and had a high affinity for hydroxyapatite. The optimized radiolabeling methods could be used to prepare the other radiohalogenated-labeled oligopeptides using ^{123}I, ^{124}I, and ^{131}I radionuclides instead of ^{125}I radionuclide for diagnosis and therapeutic agents targeting bone. However, further studies should be required before clinical stage evaluation.

Keywords: aspartic acid; carrier; peptide; radioiodination; bone metastases.

1. Introduction

Abundant growth and proliferation factors in bone provide a favorable environment for the growth and metastasis of tumors. In fact, bone is the main organ for metastasis of malignant tumors. The early detection of bone metastases has become increasingly important. Nuclear medicine imaging through bone-seeking radiopharmaceuticals enables earlier detection of bone abnormalities, including bone metastases, before the symptoms and anatomical changes occur [1,2]. The development of radiopharmaceuticals to diagnose and treat bone metastases in the early stage has progressed in recent years.

Radiopharmaceuticals, as single photon emission computed tomography (SPECT) agents such as [^{99m}Tc]Tc-methylene diphosphonate ([^{99m}Tc]Tc-MDP) and [^{99m}Tc]Tc-hydroxymethylenediphosphonate ([^{99m}Tc]Tc-HMDP), and positron emission tomography (PET) agents such as [^{18}F]NaF have been used clinically for localizing the metastatic lesion in the bone [2-4]. Meanwhile, radiopharmaceuticals for the treatment of pain from bone metastases, such as [^{153}Sm]Sm-ethylenediaminetetramethylenephosphonate ([^{153}Sm]Sm-EDTMP) and [^{89}Sr]$SrCl_2$, have been approved for the treatment of pain from all osteoblastic bone metastases [4,5].

Other radiolabeled compounds-based biphosphonate derivatives conjugated with radionuclides, such as fluorine-18 (F-18), rhenium-186, gallium-67, gallium-68, yttrium-90, and technetium-99m, have been developed [6-16]. These radiometal complexes showed excellent accumulation in the bone as an organ target and low accumulation in others and could be potential bone-seeking agents.

Poly-acidic-amino acid peptides (glutamic acid (Glu), aspartic acid (Asp), and γ-carboxyglutamic acid (Gla) have a high affinity for hydroxyapatite, and their biodistribution studies exhibited excellent carriers of radionuclide ^{67}Ga to the bone [17-22]. A previous study showed that the binding affinity of oligopeptides toward hydroxyapatite using repeated D-Asp amino acid was similar to that of L-Asp amino acid. In addition, according to biodistribution results, the accumulation of radiogallium complexes in the bone of ddY mice was comparable to that of oligopeptide with repeated D-Asp and L-Asp amino acids [18].

This study aims to develop a new radiohalogenated-labeled repeated aspartic acid amino acid for bone disorder detection. We used iodine-125 (^{125}I) radionuclide for initial studies here due to its long half-life ($t_{1/2}$ = 59.4 days). However, the radiosynthesis method developed in this study could also be applied in preparing SPECT imaging agents using iodine-123 (^{123}I), PET imaging agents using iodine-124 (^{124}I), and therapeutic probes using iodine-131 (^{131}I) radionuclides instead of the ^{125}I radionuclide. Here, we introduced radioiodine into the prosthetic group, which linked to oligopeptides with different lengths of L-Asp amino acid (n = 8 and 11) with linker caproic acid, namely [^{125}I]IB-D_8-OH ([^{125}I]**8**) or [^{125}I]IB-D_{11}-OH ([^{125}I]**9**) (Figure 1), optimized the radiosynthesis, evaluated their lipophilicity, stability, and affinity for hydroxyapatite.

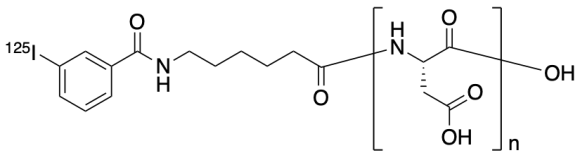

[^{125}I]**8** (n = 8)
[^{125}I]**9** (n = 11)

Figure 1. Structures of [^{125}I]IB-D_8-OH ([^{125}I]**8**) and [^{125}I]IB-D_{11}-OH ([^{125}I]**9**).

2. Materials and Methods

2.1. Materials.

[^{125}I]Sodium iodide ([^{125}I]NaI) (644 GBq/mg) was bought from PerkinElmer (Waltham, MA, USA). The commercially available chemicals and solvents were reagent grade and used as received and purchased from AmBeed, Inc. (Illinois, USA), Watanabe Chemical Industries, Ltd. (Hiroshima, Japan), Nacalai Tesque, Inc. (Kyoto, Japan), and Tokyo Chemical Industry Co., Ltd. (Tokyo, Japan). Proton nuclear magnetic resonance (^{1}H-NMR) spectra were recorded on JEOL JNM-ECS400 (JEOL Ltd, Tokyo, Japan). Low-resolution mass spectra (LRMS) were obtained by JEOL JMS-T100TD (JEOL Ltd, Tokyo, Japan). Peptides and radiolabeled compounds were purified by high-performance liquid chromatography (HPLC) (Shimadzu, Kyoto, Japan). An auto γ-counter system (Aloka Co., Ltd., Tokyo, Japan) was used to analyze the radioactivity of radiolabeled compounds.

2.2. Preparation of the reference compounds and precursors.

Reference compounds and precursors, ATE (**2**), SIB (**3**), IB-Ahx-D$_8$-OH (**8**), IB-Ahx-D$_{11}$-OH (**9**), ATE-Ahx-(Asp(O*t*Bu))$_8$-OH (**10**), ATE-Ahx-(Asp(O*t*Bu))$_{11}$-OH (**11**), were prepared in accord with the step synthesis outlined in Scheme 1.

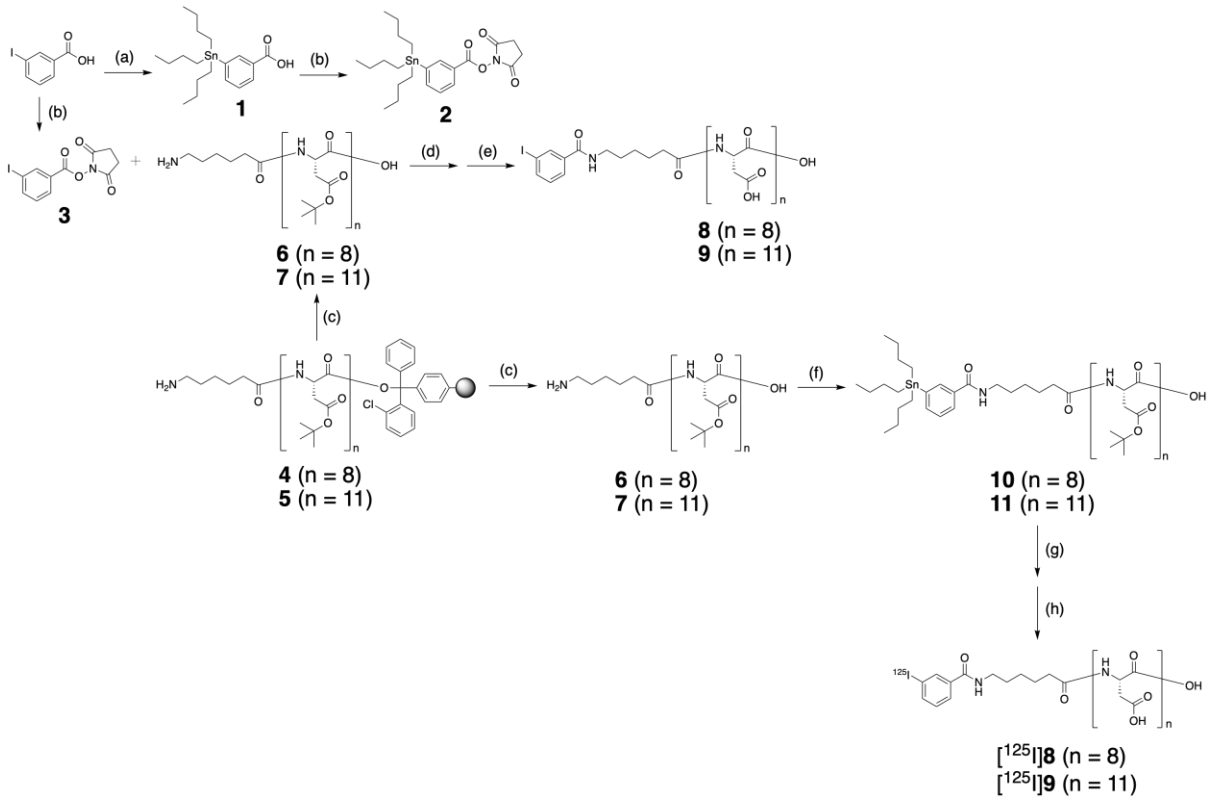

Scheme 1. Synthesis of IB-D$_8$-OH (**8**), IB-D$_{11}$-OH (**9**), [^{125}I]IB-D$_8$-OH ([^{125}I]**8**), [^{125}I]IB-D$_{11}$-OH ([^{125}I]**9**). Reagents and conditions: **(a)** hexabutyldistannane, Pd[P(C$_6$H$_5$)$_3$]$_4$, toluene; **(b)** NHS, DCC, THF anhydrous; **(c)** 30% HFIP in DCM; **(d)** DIPEA, DMF; **(e)** TFA/TIS/H$_2$O (95:2.5:2.5); **(f)** **2**, DIPEA, DMF; **(g)** [^{125}I]NaI, NCS, acetic acid, ACN; **(h)** TFA.

2.2.1. Preparation of *N*-succinimidyl 3-(tri-n-butylstannyl)benzoate (ATE) (**2**).

The bottom flask containing 3-iodobenzoate (250 mg, 1.0 mmol), hexabutyldistannane (1.0 mL, 2.0 mmol), and tetrakis(triphenylphosphine)palladium(0) (Pd[P(C$_6$H$_5$)$_3$]$_4$) (160 mg, 0.15 mmol) was added anhydrous toluene (10 mL). The mixture was refluxed overnight. After

cooling, palladium was removed by filtration using celite® [23,24]. The reaction mixture was concentrated and then purified by column chromatography using hexane: ethyl acetate (Hex: EtOAc) = 10:1) as eluent to afford the 3-(tri-N-butylstannyl)benzoic acid (**1**).

The bottom flask containing **1** (300 mg, 0.7 mmol), *N*, *N*'-dicyclohexylcarbodimide (DCC) (173 mg, 0.84 mmol), and *N*-hydroxysuccinimide (NHS) (89 mg, 0.77 mmol) was added anhydrous tetrahydrofuran (THF) (8 mL). After stirring at ambient temperature overnight, the filtrate was collected and concentrated *in vacuo*. Product *N*-succinimidyl 3-(tri-*n*-butylstannyl)benzoate (ATE) (**2**) was yielded after purification using flash column chromatography (Hex: EtOAc = 10:1) [24].

2.2.2. Preparation of *N*-succinimidyl 3-iodobenzoate (SIB) (**3**).

A mixture of 3-iodobenzoic acid (100 mg, 0.4 mmol), DCC (99 mg, 0.48 mmol), and NHS (51 mg, 0.44 mmol) in anhydrous THF (4 mL) was stirred overnight at ambient temperature. After filtration, the filtrate was collected, concentrated *in vacuo*, and purified by flash column chromatography using Hex: EtOAc (10:1) to afford **3** [23].

2.2.3. Preparation of reference compounds.

Reference compounds, IB-Ahx-$(Asp)_8$-OH (IB-D_8-OH, **8**) and IB-Ahx-$(Asp)_{11}$-OH (IB-D_{11}-OH, **9**), were prepared using a standard Fmoc-based solid-phase (SPPS) method following a previous study with some modifications [23,24]. In brief, a mixture of Fmoc-Asp(O*t*Bu)-OH (4.0 equiv), DIPEA (2.5 equiv), and 2-chlorotrityl chloride resin (1.0 equiv) in dichloromethane (DCM) was reacted at ambient temperature. After shaking for 2 hours, DCM was removed and replaced with methanol (2 mL), and the mixing was continued for another 30 minutes. The mixture was washed with DMF several times, followed by adding 20% piperidine in dimethylformamide (DMF), and the mixture was stirred for 15 minutes to deprotect the Fmoc group. After washing with DMF, the Fmoc-Asp(O*t*Bu)-OH (2.5 equiv), 1-hydroxybenzotriazole hydrate (HOBt) (2.5 equiv), and 1,3-diisopropylcarbodiimide (DIPCI) (2.5 equiv), and DMF (0.8 mL) were charged into the residue, and the mixing was continued for 2 hours. The next peptide chain was constructed following the steps (i) Fmoc deprotection by 20% piperidine for 15 minutes and (ii) coupling the amino acid (Fmoc-Asp(O*t*Bu)-OH (2.5 equiv) or Fmoc-Ahx-OH (2.5 equiv) for 2 hours with HOBt (2.5 equiv) and DIPCI (2.5 equiv) in DMF (0.8 mL). This step was repeated until the peptide length was reached, and each step of Fmoc-deprotection and peptide coupling was monitored by the Kaiser test to obtain resin-$[Asp(O\textit{t}Bu)]_8$-Ahx-NH_2 (**4**) or resin-$[Asp(O\textit{t}Bu)]_{11}$-Ahx-$NH_2$ (**5**). Subsequently, the reaction mixture was treated with 30% 1,1,1,3,3,3-hexafluoro-2-propanol (HFIP) in DCM to remove the resin. After stirring for 5 minutes at ambient temperature, crude peptides without resin, namely NH_2-Ahx-$[Asp(O\textit{t}Bu)]_8$-OH (**6**) or NH_2-Ahx-$[Asp(O\textit{t}Bu)]_{11}$-OH (**7**), were collected by filtration. After concentrating the filtrate *in vacuo*, the residue was used in the following reaction without further purification. The mixture of **6** (26 mg, 17 µmol) or **7** (34 mg, 17 µmol), **3** (9 mg, 26 µmol), and DIPEA (30 µL, 0.17 mmol) in DMF (150 µL) was reacted by stirring overnight at ambient temperature. Subsequently, the reaction was quenched by concentrating the mixture *in vacuo*. The residue was treated with a mixture of water (2.5%): triisopropylsilane (TIS) (2.5%): trifluoroacetic acid (TFA) (95%) (2 mL) to afford the reference compounds **8** or **9**. Purification of reference compounds by RP-HPLC on Cosmosil $5C_{18}$ARII column size 10 ID × 150 mm (Nacalai Tesque) with a flow rate of 4.0 mL/min for 20 minutes analysis with a

mobile phase gradient system of 50% to 70% methanol (MeOH) in water containing 0.1% TFA (system A). The chromatogram was recorded using UV absorption (254 nm wavelength). After lyophilization, white solids of **8** (10 mg; 46%) and **9** (12 mg; 43%) were collected, and then ESI-MS was used to confirm their molecular weight.

LRMS (ESI^+) m/z analysis ($[M+H]^+$) of **8** calcd for $C_{45}H_{57}IN_9O_{27}$ = 1282.2 found 1282.4.

LRMS (ESI^+) m/z analysis ($[M+H]^+$) of **9** calcd for $C_{57}H_{72}IN_{12}O_{36}$ = 1627.3 found 1627.4.

2.2.4. Preparation of precursors.

Precursors, ATE-Ahx-(Asp(O*t*Bu))$_8$-OH (**10**) and ATE-Ahx-(Asp(O*t*Bu))$_{11}$-OH (**11**), were prepared as reported in the study with some modifications [23,24]. In brief, the mixture of **6** (57 mg, 0.038 mmol) or **7** (76 mg, 0.038 mmol), DIPEA (13.2 µL, 0.38 mmol), and **2** (29 mg, 0.057 mmol) in DMF (250 µL) was reacted overnight at ambient temperature. After concentrating the reaction mixture in vacuo, the crude precursors **10** or **11** were yielded. Purification of crude precursors by HPLC on Cosmosil 5C_{18}AR-II column size 10 ID × 150 mm (Nacalai Tesque) at 4.0 mL/min flow rate with a mobile phase gradient system of 93% to 95% MeOH in water containing 0.1% TFA (system B) for 11 minutes for **10** and 94% to 96% MeOH in water containing 0.1% TFA (system C) for 11 minutes for **11**. The chromatogram was recorded using UV absorption (254 nm wavelength). After lyophilization, white solids of **10** (21 mg; 29%) and **11** (25 mg; 27%) were collected, and then ESI-MS was used to confirm their molecular weight.

LRMS (ESI^+) m/z analysis ($[M+H]^+$) of **10** calcd for $C_{89}H_{148}N_9O_{27}Sn$ = 1894.9 found 1894.9.

LRMS (ESI^+) m/z analysis ($[M+H]^+$) of **11** calcd for $C_{113}H_{187}N_{12}O_{36}Sn$ = 2409.2 found 2409.2.

2.3. Radiolabeling.

Radioiodinated compounds, [^{125}I]IB-D$_8$-OH ([^{125}I]**8**) or [^{125}I]IB-D$_{11}$-OH ([^{125}I]**9**), were prepared by an iododestannylation reaction wherein the corresponding tributylstannyl precursors (**10** or **11**) were reacted with an oxidizing agent, here we used NCS, in acid solution [24-26]. The radiotracers were purified by HPLC using a Cosmosil 5C_{18}AR-II column size 4.6 ID × 150 mm (Nacalai Tesque) at 1.0 mL/min flow rate with a gradient mobile phase of 40% to 65% MeOH in water containing 0.1% TFA for 20 minutes (system D) for [^{125}I]IB-D$_8$-OH ([^{125}I]**8**) and 40% to 60% MeOH in water containing 0.1% TFA for 20 minutes (system E) for [^{125}I]IB-D$_{11}$-OH ([^{125}I]**9**). An auto γ-counter determined the radiochemical yield and purity of radiotracers.

The precursor (**10** or **11**) in a sealed vial (1 mg/mL, 5 µL) was dissolved with 10 µL of acetonitrile (ACN), followed by the addition of acetic acid in ACN (5%, 10 µL), 2 µL [^{125}I]NaI solution in 0.1 M NaOH, and NCS in ACN (5 mg/mL, 15 µL). The mixture was reacted at various temperatures (room temperature (27°C), 40, 60, and 75°C) and various incubation times (5, 10, 15, and 20 minutes). This step was followed by removing the reaction solvent using N_2 gas and adding the TFA (100 µL). After reacting for another 30 minutes, TFA was removed by N_2 gas, and HPLC purified the residue after adding the initial mobile phase to afford [^{125}I]**8** or [^{125}I]**9**.

2.4. Evaluation of in vitro stability.

The stability of radioiodinated compounds, [^{125}I]**8** and [^{125}I]**9**, in phosphate-buffered saline (PBS(-)) pH 7.4 and murine plasma was determined as reported in the study [27,28]. The stability test in PBS(-) (pH 7.4) was conducted by adding 25 µL of [^{125}I]**8** or [^{125}I]**9** (37 kBq) into sealed tubes and mixing with 225 µL of PBS(-). After incubation for 6 hours at 37 °C, the purity of radiotracers was analyzed by HPLC (system D for [^{125}I]**8** and system E for [^{125}I]**9**) (n = 3). In the case of the stability of [^{125}I]**8** and [^{125}I]**9** in murine plasma, 10 µL of radiotracers (74 kBq) was added into sealed tubes containing 90 µL of murine plasma. After incubation for 6 hours at 37°C, an equivalent amount of ice-cold acetonitrile was added. After centrifugation at 1000*g* at 4°C for 10 minutes, the supernatant was filtered, and HPLC was used to analyze the purity of [^{125}I]**8** and [^{125}I]**9** under the same conditions as above.

2.5. Partition coefficient determination.

The partition coefficient was determined by analyzing the distribution of [^{125}I]**8** and [^{125}I]**9** into n-octanol and 0.1 M phosphate buffer (PB) pH 7.4, following the reported study [19,29]. Each radiotracer, [^{125}I]**8** or [^{125}I]**9**, was added to n-octanol saturated with PB in a test tube. The test tube was vortexed for 1 minute and stood at ambient temperature for 10 minutes (repeated thrice). This step was followed by centrifugation of the mixture (5 minutes, 3,060*g*, 4°C). Radioactivity (RA) of each layer was determined by an auto γ-counter (n = 4). Lipophilicity (partition coefficient) was determined by calculating the logarithm of the ratio RA of n-octanol to PB.

2.6. Hydroxyapatite-binding assays.

Hydroxyapatite (HA)-binding studies were carried out based on reported procedures [21,30]. Into various weights (0.2, 0.5, 2.0, and 5.0 mg) of hydroxyapatite beads (Bio-Gel; Bio-Rad, Hercules, CA) in sealed tubes were added 50 mM Tris/HCl-buffered saline (pH 7.4). Two hundred microliters containing radiotracer, [^{125}I]**8** or [^{125}I]**9**, and 19.5 µM its non-radioiodinated compound, **8** or **9**, in 50 mM Tris/HCl-buffered saline (pH 7.4) were added to 200 µL of HA suspension followed by gently shaking (500 rpm) at room temperature for 1 hour. After centrifugation for 5 minutes at a speed of 10,000g, the RA of supernatants was determined by an auto γ-counter (n = 4). The control was conducted using the same protocol without HA beads. The HA-binding ratios were determined as follows:

$$Hydroxyapatite\ binding\ (\%) = \left(1 - \frac{sample\ supernatant\ RA}{control\ supernatant\ RA}\right) x100\% \quad (1)$$

3. Results and Discussion

3.1. Synthesis of the reference compounds and precursors.

The non-radioactive iodinated compounds as reference compounds, IB-Ahx-$(Asp)_8$-OH (IB-D_8-OH, **8**) and IB-Ahx-$(Asp)_{11}$-OH (IB-D_{11}-OH, **9**), were easily yielded according to Scheme 1. There were three steps in preparing these compounds. After synthesizing the prosthetic moiety (SIB) and the oligopeptide, these compounds were conjugated in basic conditions, followed by removing the protecting groups.

The SIB (**3**) was synthesized by reacting 3-iodobenzoic acid with DCC and NHS under stirring overnight. The DCC reacts with a carboxylic group of 3-iodobenzoic acid to form the activated intermediate, *O*-acylisourea, which is more reactive than the original carboxylic acid. The *O*-acylisourea intermediate further reacts with NHS to form an NHS ester. The NHS ester is then highly reactive to the amine groups of oligopeptides, forms an amide bond, and releases NHS [31]. After purification by column chromatography with hexane: ethyl acetate (10: 1) as the eluent, **3** was yielded as a colorless solid as a colorless solid (120 mg, 87%) [24]. The ^{1}H-NMR spectrum (400 MHz, $CDCl_3$): δ 2.92 (4H, s), 7.25 – 7.30 (1H, m), 8.00 – 8.03 (1H, m), 8.09 – 8.12 (1H, m), 8.47 (1H, s) (Figure 2).

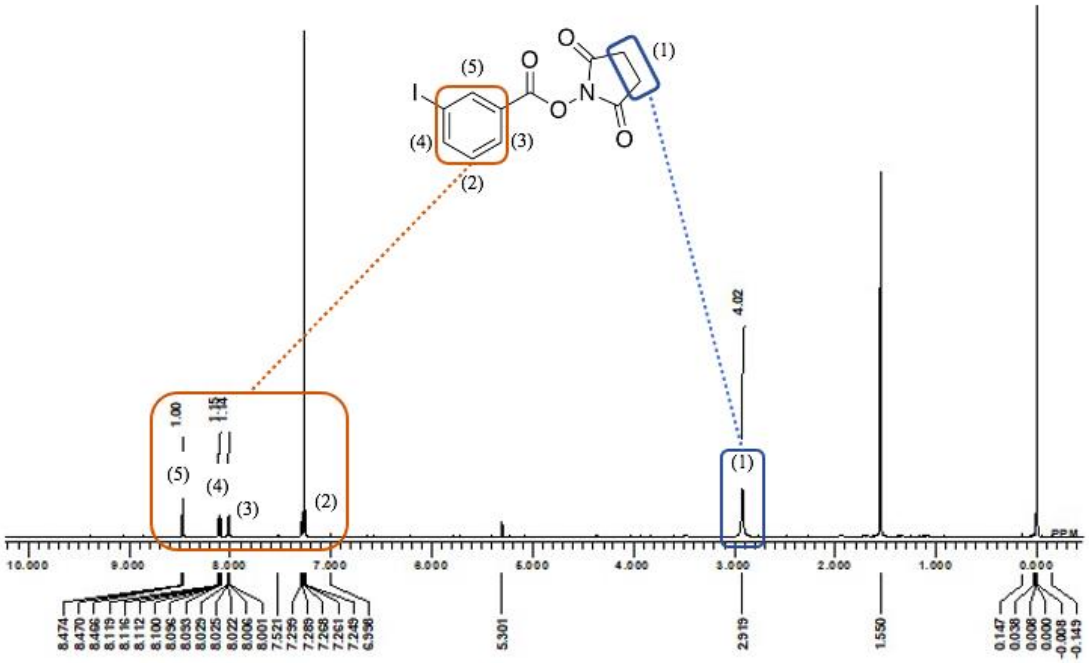

Figure 2. ^{1}H-NMR: *N*-succinimidyl 3-iodobenzoate ($CDCl_3$).

Oligo-aspartic acids were prepared using the SPPS method. Compared to LPPS (liquid-phase peptide synthesis), the SPPS method is faster, more efficient with a small amount of byproduct, and more economical than LPPS. Some of the advantages of SPPS include: (1) washing away excess reagents and products can be easy, (2) utilizing an excess of reagents could speed up and complete the reactions, (3) characterizing the intermediate compounds is not necessary, Kaiser test can be used to confirm the reaction progress, (4) availability of a larger variety of highly polar and low volatility solvents, (5) by creating a "pseudo-dilute" microenvironment, the tethered peptide can prevent intermolecular reactions which facilitates some modifications, and (6) appropriateness for automated synthesis technology. The oligopeptide-linker conjugate, namely NH_2-Ahx-[Asp(O*t*Bu)]$_8$-OH (**6**) or NH_2-Ahx-[Asp(O*t*Bu)]$_{11}$-OH (**7**), which was prepared by SPPS, was then reacted with SIB (**3**) in DMF at ambient temperature. In this study, we used DIPEA to adjust the solution pH to activate the amine group of the oligopeptide conjugate linker (hexanoic acid). DIPEA is easy to evaporate compared to the basic buffer, which is usually used to adjust the pH of the solution to basic. After conjugation of protected oligopeptide and SIB, the protecting groups of oligopeptides were removed using an acidic solution mixture H_2O/TIS/TFA (2.5:2.5:95). After purification by HPLC (system A), the isolated compounds then be lyophilized using freeze-drier, to yield the non-radioactive compounds **8** (46%) and **9** (43%) (Scheme 1). The structures of the non-radioactive iodinated compounds, **8** and **9**, were characterized by ESI-MS (Figure 3c and d). The LRMS ESI spectra **8** showed $[M + H]^+$ ion peak at m/z 1282.4 and **9** at 1627.4.

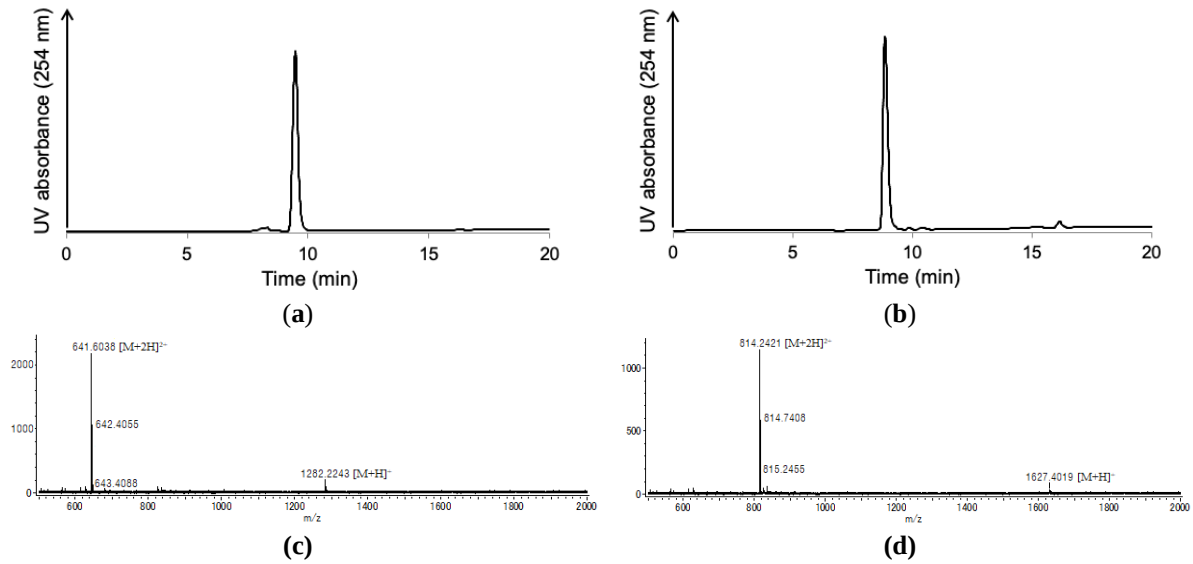

Figure 3. HPLC chromatograms of reference compounds for **(a)** IB-D_8-OH **(8)**; **(b)** IB-D_{11}-OH **(9)**. Condition: mobile phase of 40% to 60% MeOH in water with 0.1% TFA for **8** minutes and 40% to 65% MeOH in water with 0.1% TFA for **9** to 20 minutes at a 1 mL/min flow rate. The ESI-MS spectra for **(c) 8** with $[M + H]^+$ ion peak at m/z 1282.4 amu; **(d) 9** with $[M + H]^+$ ion peak at m/z 1627.4 amu.

N-succinimidyl 3-(tri-n-butylstannyl)benzoate (ATE) was used for synthesizing precursors **10** and **11**. The ATE-conjugated peptides [32] or small molecules [23,33] were commonly used as precursors for their radioiodinated compounds. After introducing the tri-butyl tin moiety as the leaving group into 3-iodobenzoic acid instead of iodine by utilizing the Pd(0) catalyst, the intermediate compound 3-(tri-*N*-butylstannyl)benzoic acid (**1**) was obtained as a colorless oil in 324 mg or 79% yield. The ^{1}H-NMR spectrum (400 MHz, $CDCl_3$): δ 0.86 – 0.94 (9H, m), 1.01 – 1.77 (18H, m), 7.36 – 7.44 (1H, m), 7.64 – 7.71 (1H, m), 7.98 – 8.03 (1H, m), 8.15 – 8.19 (1H, m) (Figure 4). Furthermore, the product *N*-succinimidyl 3-(tri-n-butylstannyl)benzoate (ATE) (**2**) was then obtained after reacting the 3-(tri-*N*-butylstannyl)benzoic acid (**1**) and DCC and NHS under stirring overnight as a colorless oil. The ^{1}H-NMR spectrum (400 MHz, DMSO-d_6): δ 0.82 – 0.91 (9H, m), 1.01 – 1.18 (6H, m), 1.23 – 1.33 (6H, m), 1.42 – 1.59 (6H, m), 2.88 (4H, s), 7.58 – 7.62 (1H, m), 7.88 – 7.90 (1H, m), 8.01 (1H, dd, J = 7.6, 2.0 Hz), 8.13 (1H, d, J = 0.8 Hz) (Figure 5).

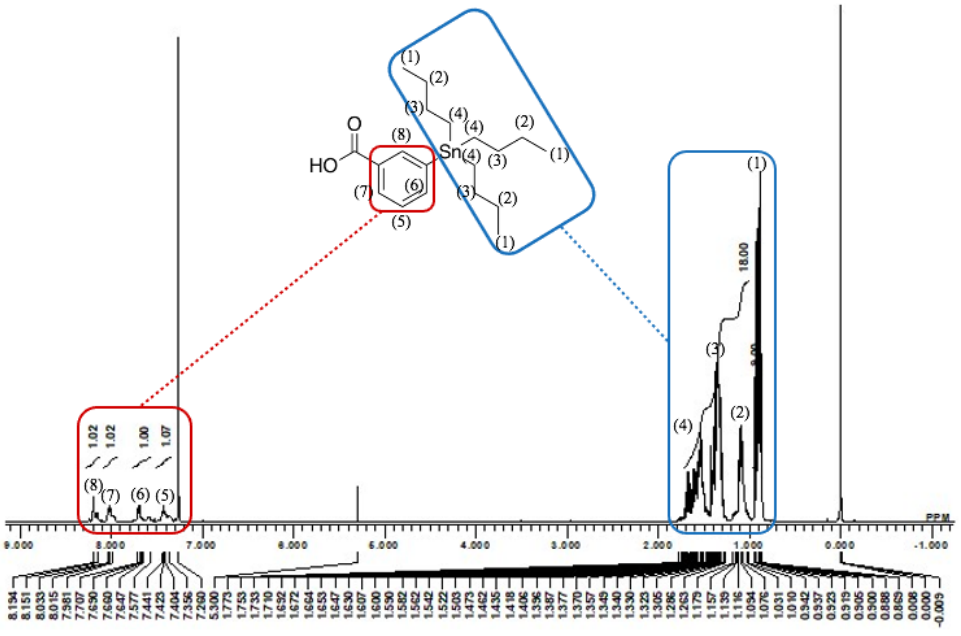

Figure 4. ^{1}H-NMR: 3-(tri-*N*-butylstannyl)benzoic acid ($CDCl_3$).

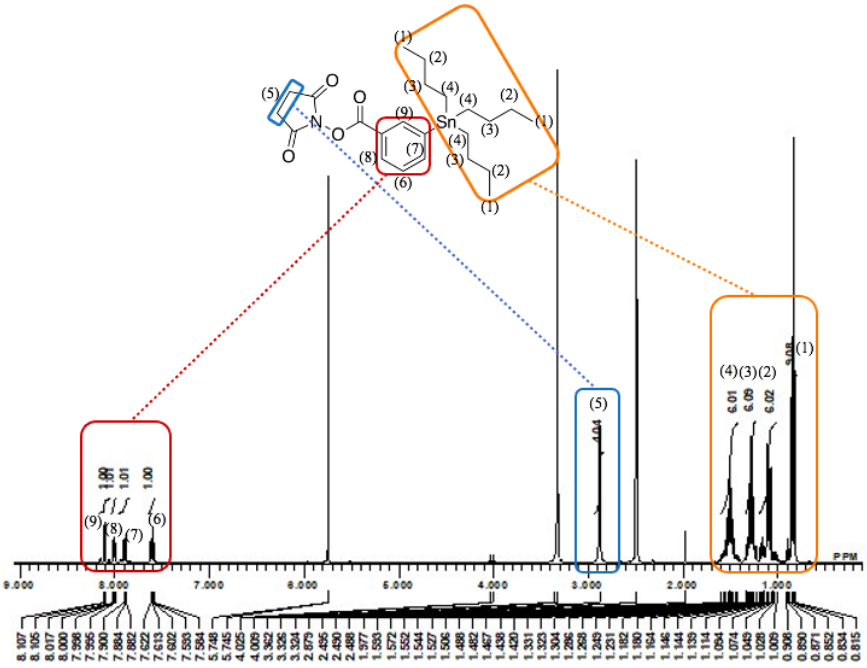

Figure 5. ^{1}H-NMR: *N*-succinimidyl 3-(tri-n-butylstannyl)benzoate (DMSO-d_6).

For the synthesis of tin precursors **10** and **11**, the synthesized ATE was reacted with **6** and **7** with chemical yields of 29% and 27%, respectively. The preparation of **10** and **11** using a similar protocol in synthesizing **8** and **9** without removing the protecting group of aspartic acid because tin compounds were not stable in the TFA solution.

3.2. Synthesis of radiolabeled compounds.

Two novel ^{125}I-labeled oligo-aspartic acids, namely [^{125}I]IB-D$_8$-OH ([^{125}I]**8**) or [^{125}I]IB-D$_{11}$-OH ([^{125}I]**9**) (Figure 6), were prepared by an iododestannylation mechanism wherein the tin group of the corresponding tributyltin precursors becomes the leaving group to be replaced by radionuclide I-125. This reaction used NCS as an oxidizing agent in an acidic condition at an optimized reaction. The identity of [^{125}I]**8** and [^{125}I]**9** was confirmed by comparing the retention times with the non-radioactive compounds **8** and **9**, respectively. Retention times for compounds **8** and [^{125}I]**8** on the RP-HPLC system D were 9.51 and 9.48 minutes, respectively. Meanwhile, the retention time for compounds **9** and [^{125}I]**9** on the RP-HPLC system E was 8.83 and 8.88 minutes, respectively. These results showed that we successfully synthesized the radioiodinated compounds according to the retention time of radiotracers, comparable to their reference compounds' retention time.

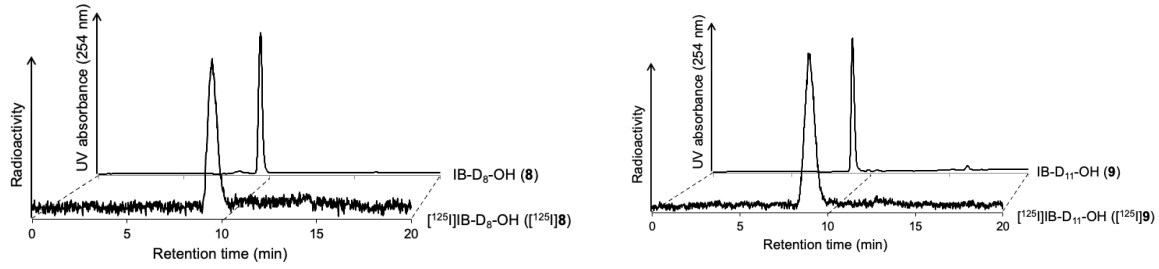

(**a**) (**b**)

Figure 6. HPLC chromatograms of **(a) 8** and [^{125}I]**8**; and **(b) 9** and [^{125}I]**9**. Condition: mobile phase of 40% to 60% MeOH in water with 0.1% TFA (for **8** and [^{125}I]**8**) and 40% to 65% MeOH in water with 0.1% TFA (for **9** and [^{125}I]**9**) for 20 minutes with a flow rate was 1 mL/min.

Various reaction times (5, 10, 15, and 20 minutes), which were performed at room temperature, affected the labeling efficiency. To optimize the labeling in this study, we used 37 kBq [^{125}I]NaI each time. After reacting the mixture at room temperature for 5 and 10 minutes, the labeling efficiency for [^{125}I]**8** was 42.3 ± 10.7% and 55.7 ± 4.0%, respectively, and for [^{125}I]**9** was 41.7 ± 7.5% and 54.0 ± 1.7%, respectively. Meanwhile, the highest labeling efficiency was reached after reacting the mixture at room temperature for 15 minutes. There are 94.3 ± 0.5% for [^{125}I]**8** and 95.3 ± 0.5% for [^{125}I]**9**. Prolonging reaction time by more than 15 minutes decreased. The labeling efficiency dropped to 93.3 ± 0.5% for both [^{125}I]**8** and [^{125}I]**9**. These results suggest we react to the mixture for 15 minutes (Figure 7). Different temperatures (room temperature (27°C), 40°C, 60°C, and 75°C) also affected the labeling efficiency. The radiolabeling efficiency after heating is lower than that at room temperature. After heating, other byproducts were formed, which were hardly found when radiolabeled compounds were heated at room temperature. Therefore, 15 minutes and room temperature were chosen as optimized radiolabeling conditions because these conditions met the highest labeling efficiency. After purification by HPLC, the radiochemical purities were over 98%.

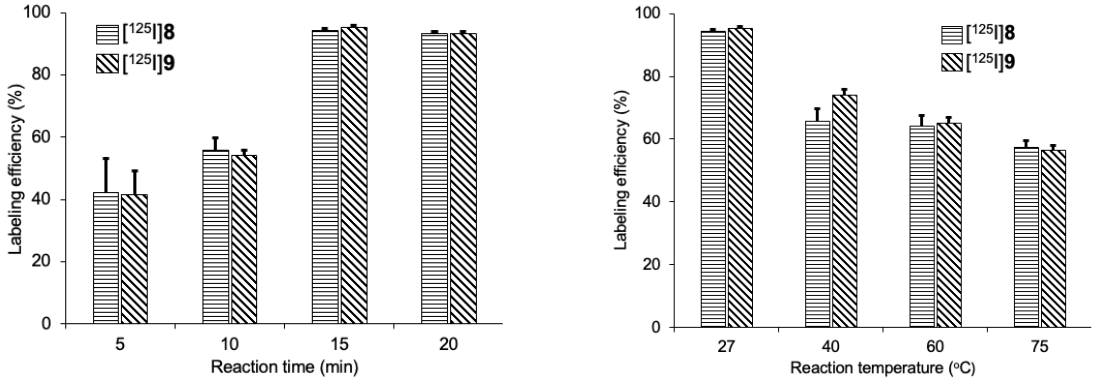

Figure 7. Radiochemical purities of [^{125}I]**8** and [^{125}I]**9** at **(a)** various reaction temperatures; **(b)** various reaction times.

3.3. Evaluation of in vitro stability.

The stability of radiotracers in PBS(-) (pH 7.4) was evaluated using HPLC analysis. After incubation for 6 hours at 37°C, [^{125}I]**8** and [^{125}I]**9** showed relatively high stability, wherein their purities remained high, more than 90%. The purities of radiotracers after 6 hours of incubation in PBS(-) (pH 7.4) were 95.9 ± 0.2% of [^{125}I]**8** and 96.1 ± 0.4% of [^{125}I]**9** (mean ± SD for three samples). In addition, the purities of [^{125}I]**8** and [^{125}I]**9** after incubation for 6 hours in murine plasma were 93.5 ± 0.4% and 95.2 ± 0.3%, respectively (mean ± SD for three samples). High remained intact after incubation, indicating that [^{125}I]**8** and [^{125}I]**9** remain stable *in vitro*.

3.4. Evaluation of partition coefficient.

The partition coefficient (log *P*) of the radioiodinated compounds was analyzed using the shake flask method by the equilibrium distribution in a mixture of an organic layer, namely n-octanol, and an organic layer, namely 0.1M phosphate buffer (PB) pH 7.4. Log P values of both radiotracers were displayed in Table 1. The funding result exhibited that the [^{125}I]**9** was more hydrophilic than the [^{125}I]**8**.

Table 1. The partition coefficient (log *P*) value of [^{125}I]**8** and [^{125}I]**9**.

Compounds	Log *P* (n-octanol/PB)
[^{125}I]IB-D_8-OH ([^{125}I]**8**)	-2.20 ± 0.08
[^{125}I]IB-D_{11}-OH ([^{125}I]**9**)	-2.42 ± 0.11

3.5. Affinity to hydroxyapatite.

Protein and inorganic crystals are combined to form bone. The mineral phase, hydroxyapatite, is composed primarily of calcium and phosphate crystals [34]. Radiotracers with excellent affinity for bone are expected to shorten the interval between injection and bone imaging. The high affinity of radiolabeled compounds for hydroxyapatite correlates with high accumulation in the bone [30,35]. Thus, we evaluated the hydroxyapatite binding of [^{125}I]**8** and [^{125}I]**9** as an index of bone affinity *in vitro* [30]. In a 0.5 mg/mL suspension, the percentage of [^{125}I]**8** and [^{125}I]**9** binding to hydroxyapatite was found to be 57.8 ± 2.6% and 55.2 ± 3.6%, respectively. This binding affinity tends to increase in line with an increasing hydroxyapatite amount and reached 91.3 ± 0.4% and 91.1 ± 0.3% for [^{125}I]**8** and [^{125}I]**9,** respectively, at 12.5 mg/mL suspension of hydroxyapatite. Both radiotracers exhibited comparable binding ratios to the hydroxyapatite (Figure 8). These findings were consistent with radiogallium-labeled oligo-aspartic acid with lengths of amino acid chains 8 and 11 [17,18,21]. Repeating aspartic acid sequences in osteopontin and glutamic acid sequences in bone sialoprotein are two dominant noncollagenous bone matrix proteins offering potential hydroxyapatite-binding sites. Poly-acid amino acids exhibit a high affinity for hydroxyapatite and could be applied as drug carriers targeting bone [17]. The findings of these initial studies, wherein [^{125}I]**8** and [^{125}I]**9** showed a high affinity for hydroxyapatite, could potentially be the carrier for radiohalogenated compounds targeting bone.

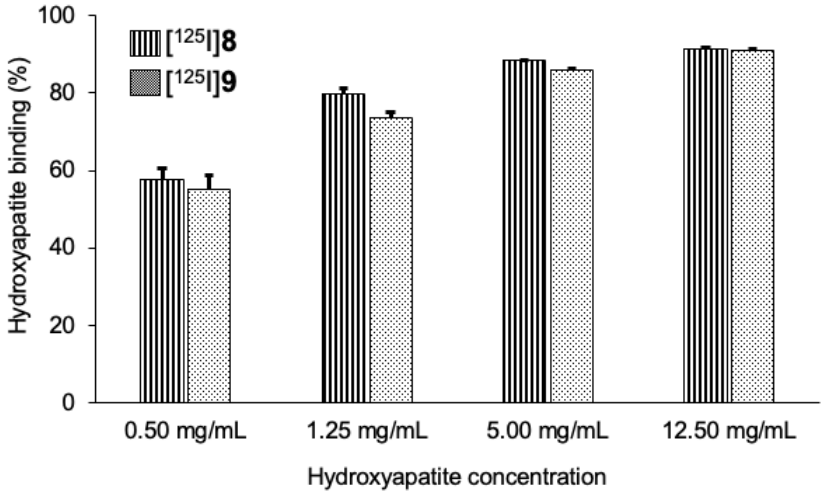

Figure 8. Hydroxyapatite binding of [^{125}I]**8** and [^{125}I]**9**. Data are expressed as the mean ± SD for four samples.

The findings showed that our designed radioiodinated-conjugated oligo-aspartic acids with different lengths (n = 8 and 9) have high labeling efficiency and stability and no need for heat to introduce the radionuclide iodine. [^{125}I]**8** and [^{125}I]**9** exhibited high affinity for hydroxyapatite as the dominant mineral in the bone as an organ target in this study. This labeling method could be used in preparing radioiodinated compounds-based small molecules and oligopeptides using I-123, I-124, and I-131 instead of I-125 for diagnosis and therapeutic agents targeting bone. However, this result still needs to be evaluated *in vivo* using ddY mice and a bone metastasis mouse model to confirm their accumulation in bone.

4. Conclusions

This study successfully prepared ^{125}I-labeled poly-aspartic acid peptides, which target bone using an iododestannylation reaction under non-carrier-added conditions. After optimizing the reaction conditions, [^{125}I]**8** and [^{125}I]**9** were achieved with high radiochemical yields and purities. These radioiodinated compounds were stable in PBS and murine plasma and had a high affinity for hydroxyapatite. The optimized radiolabeling methods could be used to prepare the other radiohalogenated-labeled oligopeptides using ^{123}I, ^{124}I, and ^{131}I radionuclides instead of ^{125}I radionuclide for diagnosis and therapeutic agents targeting bone. However, further studies should be required prior to clinical stage evaluation.

Author Contributions

Conceptualization, N.E.; methodology, N.E. and S.S.; validation, N.E., K.O., and A.R.; formal analysis, S.S.; investigation, S.S. and N.E.; resources, N.E., F.F., and K.O.; writing—original draft preparation, N.E. and S.S.; writing—review and editing, N.E., A.R., F.F., R.R., A.N., and K.O.; visualization, S.S.; supervision, N.E. and K.O.; project administration, N.E.; funding acquisition, N.E. and K.O. All authors have read and agreed to the published version of the manuscript.

Institutional Review Board Statement

Not applicable.

Informed Consent Statement

Not applicable.

Data Availability Statement

The original contributions presented in the study are included in the article, further inquiries can be directed to the corresponding author.

Funding

This research was funded by The Research Grant Directorate for Resources, The Ministry of Education and Culture of The Republic of Indonesia through Post Doctoral Grant, grant number 2835/E4/DV.05.03/2022 and Program Hibah PTM-DRTPM 2024 by Ministry of Research, Technology and Higher Education, Indonesia grant number 650/LL9/PK.00.PG/2024, 2250/B.07/UMI/VI/2024.

Acknowledgments

The authors are grateful to the Clinical and Analytical Science Laboratory – Kanazawa University authorities for accommodating the necessary facilities to conduct this research.

Conflicts of Interest

The authors declare no conflict of interest.

References

1. Ogawa, K.; Ishizaki, A. Well-Designed Bone-Seeking Radiolabeled Compounds for Diagnosis and Therapy of Bone Metastases. *Biomed. Res. Int.* **2015**, *2015*, 676053, https://doi.org/10.1155/2015/676053.
2. Costelloe, C.M.; Lin, P.P.; Chuang, H.H.; Amini, B.; Chainitikun, S.; Yu, T.-K.; Ueno, N.T.; Murphy, W.A.; Madewell, J.E. Bone Metastases: Mechanisms of the Metastatic Process, Imaging and Therapy. *Semin. Ultrasound CT MRI* **2021**, *42*, 164-183, https://doi.org/10.1053/j.sult.2020.08.016.
3. Subramanian, G.; McAfee, J.G.; Blair, R.J.; Kallfelz, F.A.; Thomas, F.D. Technetium-99m-methylene diphosphonate--a superior agent for skeletal imaging: comparison with other technetium complexes. *J. Nucl. Med.* **1975**, *16*, 744-755.
4. Şanli, Y. Radionuclide Therapy in the Treatment of Bone Metastases. *Turk. J. Oncol.* **2021**, *36*, 48-53, https://doi.org/10.5505/tjo.2021.S1012.
5. Mishra, S.G.; Sawant, D.K.; Chindarkar, A.S.; Thamke, A.N.; Sanjeev Kumar, B.; Dey, A.C.; Kulkani, M.S. Europium radionuclides in samarium-153-Ethylene Diamine Tetramethylene phosphonic acid (^{153}Sm-EDTMP) radiopharmaceutical waste. *Appl. Radiat. Isot.* **2022**, *188*, 110386, https://doi.org/10.1016/j.apradiso.2022.110386.
6. Ogawa, K.; Mukai, T.; Arano, Y.; Ono, M.; Hanaoka, H.; Ishino, S.; Hashimoto, K.; Nishimura, H.; Saji, H. Development of a Rhenium-186-Labeled MAG3-Conjugated Bisphosphonate for the Palliation of Metastatic Bone Pain Based on the Concept of Bifunctional Radiopharmaceuticals. *Bioconjugate Chem.* **2005**, *16*, 751-757, https://doi.org/10.1021/bc040249w.
7. Palma, E.; Oliveira, B.L.; Correia, J.D.G.; Gano, L.; Maria, L.; Santos, I.C.; Santos, I. A new bisphosphonate-containing ^{99m}Tc(I) tricarbonyl complex potentially useful as bone-seeking agent: synthesis and biological evaluation. *J. Biol. Inorg. Chem.* **2007**, *12*, 667-679, https://doi.org/10.1007/s00775-007-0215-0.
8. Uehara, T.; Jin, Z.L.; Ogawa, K.; Akizawa, H.; Hashimoto, K.; Nakayama, M.; Arano, Y. Assessment of ^{186}Re chelate-conjugated bisphosphonate for the development of new radiopharmaceuticals for bones. *Nucl. Med. Biol.* **2007**, *34*, 79-87, https://doi.org/10.1016/j.nucmedbio.2006.10.001.
9. Ogawa, K.; Kawashima, H.; Shiba, K.; Washiyama, K.; Yoshimoto, M.; Kiyono, Y.; Ueda, M.; Mori, H.; Saji, H. Development of [^{90}Y]DOTA-conjugated bisphosphonate for treatment of painful bone metastases. *Nucl. Med. Biol.* **2009**, *36*, 129-135, https://doi.org/10.1016/j.nucmedbio.2008.11.007.
10. Mukai, T.; Ogawa, K.; Arano, Y.; Ono, M.; Fujioka, Y.; Izumo, M.; Konishi, J.; Saji, H. Synthesis and evaluation of bisphosphonate derivative labeled with rhenium-186 using monoaminemonoamide-dithiols as a chelating group. *J. Label. Compd. Radiopharm.* **2001**, *44*, S617-S618, https://doi.org/10.1002/jlcr.25804401218.
11. Ashhar, Z.; Yusof, N.A.; Ahmad Saad, F.F.; Mohd Nor, S.M.; Mohammad, F.; Bahrin Wan Kamal, W.H.; Hassan, M.H.; Ahmad Hassali, H.; Al-Lohedan, H.A. Preparation, Characterization, and Radiolabeling of [^{68}Ga]Ga-NODAGA-Pamidronic Acid: A Potential PET Bone Imaging Agent. *Molecules* **2020**, *25*, 2668, https://doi.org/10.3390/molecules25112668.
12. Keeling, G.P.; Sherin, B.; Kim, J.; San Juan, B.; Grus, T.; Eykyn, T.R.; Rösch, F.; Smith, G.E.; Blower, P.J.; Terry, S.Y.A.; T. M. de Rosales, R. [^{68}Ga]Ga-THP-Pam: A Bisphosphonate PET Tracer with Facile Radiolabeling and Broad Calcium Mineral Affinity. *Bioconjugate Chem.* **2021**, *32*, 1276-1289, https://doi.org/10.1021/acs.bioconjchem.0c00401.
13. Hassan, H.; Othman, M.F.; Abdul Razak, H.R.; Zakaria, Z.A.; Ahmad Saad, F.F.; Osman, M.A.; Yi, L.H.; Ashhar, Z.; Idris, J.; Abdul Hamid, M.H.; Safee, Z.M. Preparation, Optimisation, and In Vitro Evaluation of [^{18}F]AlF-NOTA-Pamidronic Acid for Bone Imaging PET. *Molecules* **2022**, *27*, 7969, https://doi.org/10.3390/molecules27227969.
14. Xiao, D.; Jiang, Y.; Feng, J.; Ruan, Q.; Wang, Q.; Yin, G.; Zhang, J. Novel ^{99m}Tc labeled complexes with bisphosphonate isocyanide: Radiosynthesis and evaluation as potential bone-seeking agents. *Bioorg. Med. Chem. Lett.* **2022**, *73*, 128918, https://doi.org/10.1016/j.bmcl.2022.128918.
15. Ekinci, M.; Özdemir, D.İ.; Özgenç, E.; Gündoğdu, E.; AŞIkoĞLu, M. Radiolabeling, Quality Control, and Cell Binding Studies of New ^{99m}Tc-Labeled Bisphosphonates: ^{99m}Tc-Ibandronate Sodium. *Turk. J. Pharm. Sci.* **2023**, *20*, 91-99, https://doi.org/10.4274/tjps.galenos.2022.01346.
16. Keeling, G.P.; Baark, F.; Katsamenis, O.L.; Xue, J.; Blower, P.J.; Bertazzo, S.; T. M. de Rosales, R. ^{68}Ga-bisphosphonates for the imaging of extraosseous calcification by positron emission tomography. *Sci. Rep.* **2023**, *13*, 14611, https://doi.org/10.1038/s41598-023-41149-7.

17. Ogawa, K.; Ishizaki, A.; Takai, K.; Kitamura, Y.; Kiwada, T.; Shiba, K.; Odani, A. Development of Novel Radiogallium-Labeled Bone Imaging Agents Using Oligo-Aspartic Acid Peptides as Carriers. *PLoS One* **2013**, *8*, e84335, https://doi.org/10.1371/journal.pone.0084335.
18. Ogawa, K.; Ishizaki, A.; Takai, K.; Kitamura, Y.; Makino, A.; Kozaka, T.; Kiyono, Y.; Shiba, K.; Odani, A. Evaluation of Ga-DOTA-(D-Asp)$_n$ as bone imaging agents: D-aspartic acid peptides as carriers to bone. *Sci. Rep.* **2017**, *7*, 13971, https://doi.org/10.1038/s41598-017-14149-7.
19. Ishizaki, A.; Mishiro, K.; Shiba, K.; Hanaoka, H.; Kinuya, S.; Odani, A.; Ogawa, K. Fundamental study of radiogallium-labeled aspartic acid peptides introducing octreotate derivatives. *Ann. Nucl. Med.* **2019**, *33*, 244-251, https://doi.org/10.1007/s12149-018-01326-5.
20. Ogawa, K. Development of Diagnostic and Therapeutic Probes with Controlled Pharmacokinetics for Use in Radiotheranostics. *Chem. Pharm. Bull.* **2019**, *67*, 897-903, https://doi.org/10.1248/cpb.c19-00274.
21. Ogawa, K.; Nishizawa, K.; Mishiro, K.; Effendi, N.; Fuchigami, T.; Munekane, M.; Wakabayashi, H.; Kinuya, S. Synthesis and Evaluation of Radiogallium Labeled Bone-Imaging Probes Using Oligo-γ-Carboxy Glutamic Acid Peptides as Carriers to Bone. *Mol. Pharmaceutics* **2024**, *21*, 2375-2382, https://doi.org/10.1021/acs.molpharmaceut.3c01156.
22. Ogawa, K.; Nishizawa, K.; Mishiro, K.; Munekane, M.; Fuchigami, T.; Echigo, H.; Wakabayashi, H.; Kinuya, S. Differences in the Renal Accumulation of Radiogallium-Labeled (Glu)$_{14}$ Peptides Containing Different Optical Isomers of Glutamic Acid. *Molecules* **2024**, *29*, 3993, https://doi.org/10.3390/molecules29173993.
23. Effendi, N.; Ogawa, K.; Mishiro, K.; Takarada, T.; Yamada, D.; Kitamura, Y.; Shiba, K.; Maeda, T.; Odani, A. Synthesis and evaluation of radioiodinated 1-{2-[5-(2-methoxyethoxy)-1*H*-benzo[*d*]imidazol-1-yl]quinolin-8-yl}piperidin-4-amine derivatives for platelet-derived growth factor receptor β (PDGFRβ) imaging. *Bioorg. Med. Chem.* **2017**, *25*, 5576-5585, https://doi.org/10.1016/j.bmc.2017.08.025.
24. Elghobary, M.E.N.; Munekane, M.; Mishiro, K.; Fuchigami, T.; Ogawa, K. Preparation and Evaluation of Thermosensitive Liposomes Encapsulating I-125-Labeled Doxorubicin Derivatives for Auger Electron Therapy. *Molecules* **2023**, *28*, 1864, https://doi.org/10.3390/molecules28041864.
25. Echigo, H.; Mishiro, K.; Fuchigami, T.; Shiba, K.; Kinuya, S.; Ogawa, K. Synthesis and Evaluation of a Dimeric RGD Peptide as a Preliminary Study for Radiotheranostics with Radiohalogens. *Molecules* **2021**, *26*, 6107, https://doi.org/10.3390/molecules26206107.
26. Mishiro, K.; Nishii, R.; Sawazaki, I.; Sofuku, T.; Fuchigami, T.; Sudo, H.; Effendi, N.; Makino, A.; Kiyono, Y.; Shiba, K.; Taki, J.; Kinuya, S.; Ogawa, K. Development of Radiohalogenated Osimertinib Derivatives as Imaging Probes for Companion Diagnostics of Osimertinib. *J. Med. Chem.* **2022**, *65*, 1835-1847, https://doi.org/10.1021/acs.jmedchem.1c01211.
27. Effendi, N.; Mishiro, K.; Shiba, K.; Kinuya, S.; Ogawa, K. Development of Radiogallium-Labeled Peptides for Platelet-Derived Growth Factor Receptor *β* (PDGFR*β*) Imaging: Influence of Different Linkers. *Molecules* **2021**, *26*, 41, https://doi.org/10.3390/molecules26010041.
28. Effendi, N.; Mishiro, K.; Wakabayashi, H.; Gabryel-Skrodzka, M.; Shiba, K.; Taki, J.; Jastrząb, R.; Kinuya, S.; Ogawa, K. Synthesis and evaluation of radiogallium-labeled long-chain fatty acid derivatives as myocardial metabolic imaging agents. *PLOS ONE* **2021**, *16*, e0261226, https://doi.org/10.1371/journal.pone.0261226.
29. Grus, T.; Lahnif, H.; Bausbacher, N.; Miederer, M.; Rösch, F. DOTA Conjugate of Bisphosphonate and PSMA-Inhibitor: A Promising Combination for Therapy of Prostate Cancer Related Bone Metastases. *Front. Nucl. Med.* **2022**, *2*, 892147, https://doi.org/10.3389/fnume.2022.892147.
30. Hirata, S.; Mishiro, K.; Higashi, T.; Fuchigami, T.; Munekane, M.; Arano, Y.; Kinuya, S.; Ogawa, K. Synthesis and evaluation of a multifunctional probe with a high affinity for prostate-specific membrane antigen (PSMA) and bone. *Nucl. Med. Biol.* **2022**, *114-115*, 34-41, https://doi.org/10.1016/j.nucmedbio.2022.08.004.
31. Singh, A.; Sharma, A.; Chawla, P.A. The Catalyst's Companion: *N,N'*-Dicyclohexylcarbodiimide (DCC) in Action. *SynOpen* **2023**, *7*, 562-565, https://doi.org/10.1055/s-0042-1751500.
32. Kondo, N.; Kato, M.; Oshima, A.; Hirano, F.; Miyazaki, A.; Temma, T. Radioiodinated Bicyclic RGD Peptide Derivatives for Enhanced Tumor Accumulation. *Pharmaceuticals* **2025**, *18*, 549, https://doi.org/10.3390/ph18040549.
33. Aoki, M.; Odani, A.; Ogawa, K. Development of radiolabeled bis(zinc(II)-dipicolylamine) complexes for cell death imaging. *Ann. Nucl. Med.* **2019**, *33*, 317-325, https://doi.org/10.1007/s12149-019-01339-8.

34. Ogawa, K.; Mukai, T.; Inoue, Y.; Ono, M.; Saji, H. Development of a Novel ^{99m}Tc-Chelate-Conjugated Bisphosphonate with High Affinity for Bone as a Bone Scintigraphic Agent. *J. Nucl. Med.* **2006**, *47*, 2042-2047.
35. Kasugai, S.; Fujisawa, R.; Waki, Y.; Miyamoto, K.-I.; Ohya, K. Selective Drug Delivery System to Bone: Small Peptide $(Asp)_6$ Conjugation. *J. Bone Miner. Res.* **2000**, *15*, 936-943, https://doi.org/10.1359/jbmr.2000.15.5.936.

Publisher's Note & Disclaimer